JST: Engineering and Technology for Sustainable Development
Vol. 31, Issue 5, November 2021, 075-080

Thermal and Mechanical Properties of Sn-8Zn-3Bi Solder Alloy

Tính chất cơ và nhiệt của hợp kim hàn Sn-8Zn-3Bi

Duong Ngoc Binh
Hanoi University of Science and Technology, Hanoi, Vietnam
Email: binh.duongngoc@hust.edu.vn

Abstract

Thermal and mechanical properties of Sn-8Zn-3Bi solder alloy on copper substrate were evaluated via measuring the melting temperature, the coefficient of thermal expansion (CTE), the tensile and shear strength of the solder joint. The measured properties of the alloy were then compared to the properties of the traditional and widely used eutectic Sn-37Pb solder alloy. The results show that the melting (liquidus) temperature of Sn-8Zn-3Bi was 195 °C, the CTE of Sn-8Zn-3Bi was 22.2×10^{-6} K^{-1} in the temperature range of 30-130 °C. At the same testing condition, both tensile and shear strength of Sn-8Zn-3Bi joints were higher than those of Sn-37Pb. The stress-strain curve indicated that the Sn-8Zn-3Bi joints were brittle whilst the Sn-37Pb joints were ductile.

Keywords: Solder alloy, thermal properties, mechanical properties

Tóm tắt

Bài báo trình bày kết quả kiểm tra một số tính chất của hợp kim hàn không độc Sn-8Zn-3Bi để đánh giá khả năng sử dụng hợp kim này thay thế cho hợp kim hàn truyền thống Sn-37Pb. Các tính chất được xác định bao gồm nhiệt độ nóng chảy, hệ số giãn nở nhiệt, giới hạn bền kéo và giới hạn bền cắt của mối hàn hợp kim. Kết quả cho thấy trong khoảng nhiệt độ làm việc từ 30-130 °C, hợp kim hàn Sn-8Zn-3Bi có hệ số giãn nở nhiệt là 22,2×10^{-6} K^{-1}. Nhiệt độ nóng chảy hoàn toàn (nhiệt độ lỏng) của hợp kim Sn-8Zn-3Bi là 195 °C. Cả giới hạn bền kéo và giới hạn bền cắt của Sn-8Zn-3Bi đều cao hơn của Sn-37Pb. Đường cong ứng suất - biến dạng cho thấy phá hủy của mối hàn sử dụng hợp kim Sn-8Zn-3Bi là phá hủy giòn so với phá hủy dẻo của mối hàn sử dụng Sn-37Pb.

Từ khóa: Hợp kim hàn, tính chất nhiệt, tính chất cơ học

1. Introduction

Legislation is driving major changes in the manufacture of electrical and electronics equipment. The most significant change is the elimination of lead from solder joints [1-3]. With the requirement to install lead-free solder processes, companies have a choice of alloys. As the selection process does not have any detailed requirement on the alloy's property (only reliability test included), some solder alloys are being used without fundamental knowledge of the alloys [4]. Consequently, some lead-free solders are commercially available but have not yet been fully characterized. Therefore, further study on such alloys remains an important issue.

When trying to identify an alternative to the current Pb-Sn solders that are widely used, it is important to ensure that the properties of the replacement solder are comparable to or superior to Pb-Sn solders. The major performance characteristics of solders that are of importance for packaging applications are manufacturability and reliability. Manufacturability describes how well a Pb-free solder fits into current packaging practices without requiring significant changes. Manufacturability involves most of the physical properties of a solder alloy relevant to soldering such as melting temperature, solderability, viscosity, density, thermal and electrical properties, corrosion and oxidation behavior, surface tension, rework-ability, and cost [5-9]. The reliability of a solder alloy for packaging is mainly dependent on the coefficient of thermal expansion, elastic modulus, yield strength, shear strength, fatigue, and creep behavior of the alloy [10-14].

The Sn-8Zn-3Bi was a commercially available solder alloy that has been used for some time. Initially, the Sn-9Zn alloy was proposed due to its safety (lead-free), availability, and low cost. The eutectic Sn-9Zn also has a low melting point suitable for use as a solder alloy in electric and electronic equipment. It also possesses the advantages of high strength, good creep resistance, and high thermal fatigue resistance [15]. However, poor wetting and non-wetting were observed in Sn-9Zn during soldering due to the poor oxidation resistance of the alloy [16]. By adding Bi

ISSN 2734-9381
https://doi.org/10.51316/jst.154.etsd.2021.31.5.11
Received: December 17, 2020; accepted: June 23, 2021

into Sn-Zn solders, the wettability and corrosion performance of Sn-Zn solders could be improved [15].

The wettability of Sn-8Zn-3Bi on copper was evaluated via measuring the contact angle of the solder alloy on the copper substrate [17]. In this work, other important properties of Sn-8Zn-3Bi alloy such as melting temperature, coefficient of thermal expansion, tensile and shear strength of the solder joint were evaluated.

2. Experiment

The copper substrate used in this study was the commercial copper foil of 1.5 mm in thickness and has a purity of 99.9%. The solder alloys used were commercially available Sn-8Zn-3Bi and Sn-37Pb.

Sn-8Zn-3Bi samples used in CTE experiment were cut from the Sn-8Zn-3Bi solder bar. It was polished to the dimension of 20 mm in length, 3 mm in width and 3 mm in thickness. CTE of samples was measured by using a Dilatometer.

Tensile and shear specimen were prepared with the copper substrate as shown in Fig. 1.

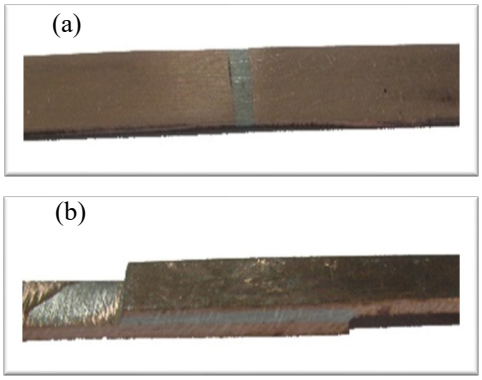

Fig. 1. a) Tensile specimen and b) Shear specimen

Copper sheet of 1.5 mm in thickness was cut in rectangular of 50 mm in length and 10 mm with. After that, the substrate was cleaned with abrasive paper and compressed air. To perform the solder joint, solder paste was loaded between two copper coupons then heated over the melting temperature of solder alloy by an electronic heater. After the solder alloy melted and spread between two copper coupons, The system is then cooled in air. The specimens obtained were cleaned to form the testing samples.

3. Results and Discussions

3.1. Melting Temperature

Fig. 2 shows the Differential Scanning Calorimetry (DSC) curve obtained from Sn-8Zn-3Bi specimen. A simple curve that shows no phase transformation of the alloy from room temperature until the melting temperature. The alloy started melting at a temperature of approx. 190 °C. The onset temperature was approx. 195 °C. The onset temperature of DSC curve can be admitted as the liquidus temperature of sample alloy [18]. Thus, the alloy's melting range was from 190 to 195 °C.

An advantage of low melting temperature solder alloy is the prevalent usage of thermoset polymers in microelectronics packaging. Epoxy resins are used for encapsulation, substrates, and attaching the silicon die to carriers or substrates, i.e., the die attach material. Currently, the highest temperatures that these polymeric materials are exposed to is approximately 230 °C for 90 s [4], during board-level assembly and/or the reflow of solder balls and solder bumps. The Sn-8Zn-3Bi which has a melting temp of 195 °C, close to the melting temperature of the traditional Sn-37Pb (183 °C) could be used as an alternative alloy in actual soldering without any change of equipment.

3.2. Coefficient of Thermal Expansion

The coefficient of thermal expansion (CTE) of Sn-8Zn-3Bi measured when temperature varies from 30 °C up to 130 °C is shown in Fig. 3.

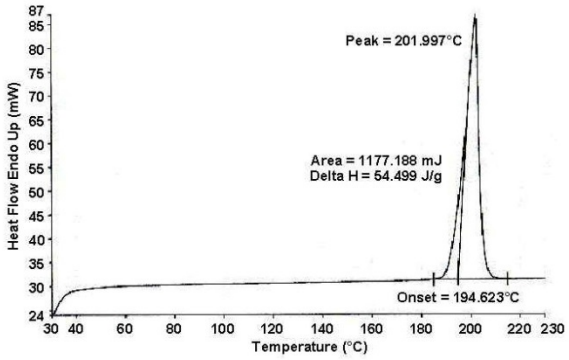

Fig. 2. DSC curve of Sn-8Zn-3Bi

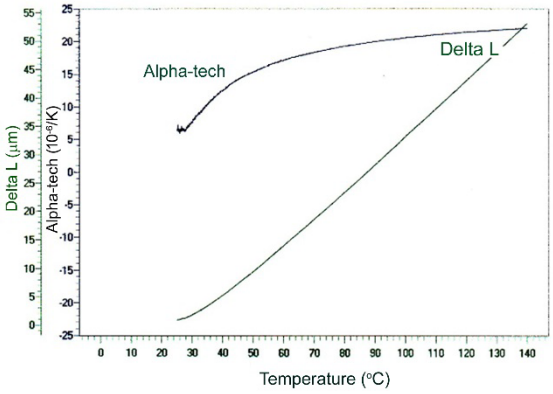

Fig. 3. Expansion of specimen (Delta L) and CTE of Sn-8Zn-3Bi

As can be seen, CTE of Sn-8Zn-3Bi alloy increased as the temperature increases up to 130 °C. Firstly, the CTE increases quite rapidly, 7.51×10^{-6} K^{-1} up to 12.53×10^{-6} K^{-1}. However, the change of CTE becomes slow at a higher temperature. The increase in sample length is almost linear up to 140 °C. In order to compare with the eutectic Sn-37Pb solder alloy, the

CTE experiment is also carried out with the traditional eutectic alloy, the obtained results are shown in Fig. 4 and Fig. 5.

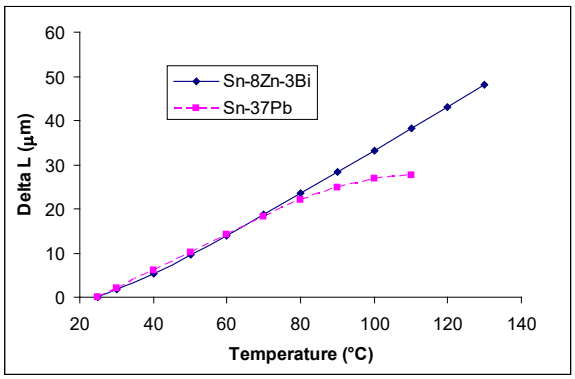

Fig. 4. Expansion of Sn-8Zn-3Bi and Sn-37Pb Specimen

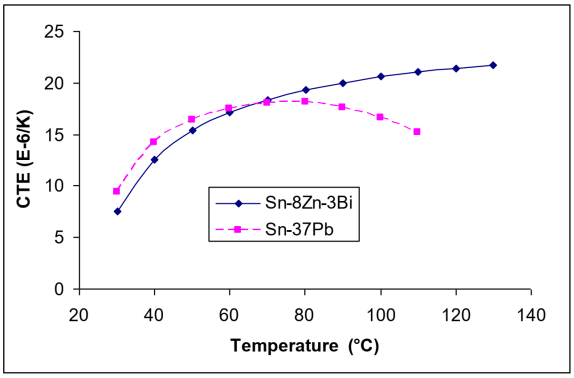

Fig. 5. CTEs of Sn-8Zn-3Bi and Sn-37Pb

The expansions in both solders are very similar up to 80 °C. However, a significant difference started at 90 °C where ΔL of Sn-8Zn-3Bi was 28.26 µm while it was 24.86 µm in Sn-37Pb. The difference of ΔL at 90 °C was 3.4 µm and it increased when temperature increases. At 110 °C (ended temperature of Sn-37Pb sample), ΔL of Sn-8Zn-3Bi sample was 38.14 µm and it was 27.56 µm in Sn-37Pb. The difference was increased to 10.58 µm.

The comparison of CTEs also shows the similarity between Sn-8Zn-3Bi and Sn-37Pb up to 80 °C (Fig. 5). Above 80 °C, the CTE of Sn-8Zn-3Bi was continued to increase as temperature increased but it was reduced in Sn-37Pb. The maximum value of CTE of Sn-37Pb was 18.07×10^{-6} K^{-1} at 80 °C and it reduced to 17.57×10^{-6} K^{-1} at 90 °C and 15.16×10^{-6} K^{-1} at 110 °C. Conversely, CTE of Sn-8Zn-3Bi kept increasing and reaches 27.41×10^{-6} K^{-1} at the ended temperature of 130 °C. CTEs of Sn-8Zn-3Bi and Sn-37Pb solder alloys are in the same range, which is close to CTE value of copper, $16\text{-}18\times10^{-6}$ K^{-1} [4].

As can be seen in Fig. 3, ΔL of Sn-8Zn-3Bi increased almost linear fit with the increasing of temperature. If we assume that the increase of ΔL is linear fit, an average value, α_L, of CTE can be calculated and can be applied through the range of temperature.

The expansion of the sample at a certain temperature can be expressed as follows:

$$\Delta L = \alpha_L L_0 \Delta T \quad (1)$$

where L_0 is the length of the sample at T_0.

From the obtained values, the equations of the linear-fit lines have been calculated:

$$\Delta L = 0.444\times10^{-6}\Delta T \quad (2)$$

From (1), (2), and $L_0 = 20$ mm we have:

$$\alpha_L = \frac{0.444\times10^{-6}}{20\times10^{-3}} = 22.2\times10^{-6}\ K^{-1}$$

These average values of CTE were used to recalculate ΔL. Results are shown in Fig. 6. As can be seen, the line of calculated values is very close to the line of measured values for Sn-8Zn-3Bi. Therefore, at the range of temperature and for engineering purposes, we can take the value 22.2×10^{-6} K^{-1} as CTE of Sn-8Zn-3Bi.

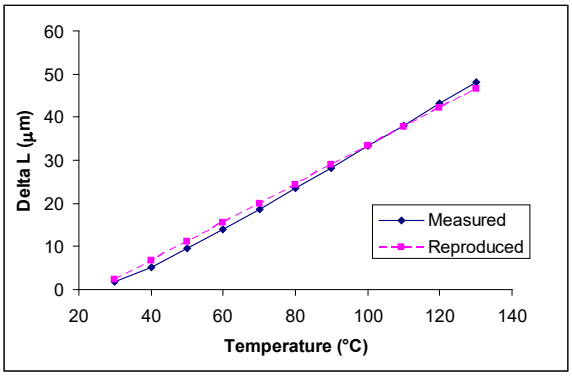

Fig. 6. $\Delta L_{measured}$ and $\Delta L_{reproduced}$ of Sn-8Zn-3Bi

3.3 Tensile Strength of the Solder Joint

Tensile strength of solder joint depends on various factors, including cooling rate [19], strain rate [20], etc... Therefore, it is difficult to have a meaningful value of tensile strength of solder alloys. For comparison, the tensile strength of Sn-8Zn-3Bi and Sn-37Pb under the same experimental conditions were measured. Results are shown in Fig. 7.

The tensile strength of Sn-8Zn-3Bi lead-free solder is higher than that of Sn-37Pb eutectic solder. The measurements at two crosshead speeds of 0.1 mm/min and 1 mm/min are shown similar results. At the first crosshead speed, 0.1 mm/min, UTS of Sn-8Zn-3Bi has a value of 36.8 MPa, 3.3 MPa higher than that of Sn-37Pb. UTS increased when crosshead speed increased, it was 47.8 MPa at a crosshead speed of 1 mm/min, 5.6 MPa higher than Sn-37Pb.

The stress-strain curve (Fig. 8) shows that the stress in Sn-8Zn-3Bi sample increased almost linearly

up to 35 MPa. The linear fit part of Sn-37Pb curve is just up to around 20 MPa. However, the Young Module (Elastic Module) of Sn-8Zn-3Bi is somewhat lower than that of Sn-37Pb.

An SEM image of the fracture surface of the Sn-8Zn-3Bi tensile specimen is shown in Fig. 9. The fracture surface can be divided into two areas, the brittle area at the edge of the specimen and the dimple pattern typical in overstress fracture of ductile material in the center of the specimen.

The result indicates that the failure is in brittle manner at the edge while it is ductile in the center of the solder joint. There is no significant plastic deformation before failure as the stress in the stress-strain curve reduced vertically when the Sn-8Zn-3Bi sample break (Fig. 8). Brittle failure was the principal failure of the Sn-8Zn-3Bi sample. Since the testing specimen was allowed to cool in the air, a fast cooling rate at the outer side of the specimen might have caused the embrittlement. Reducing the cooling rate could have eliminated the brittle phenomena of the joint.

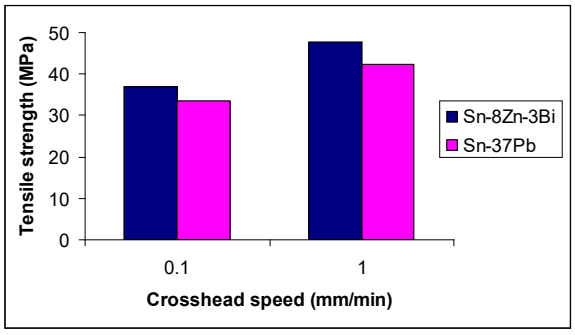

Fig. 7. Tensile strengths of solder alloys

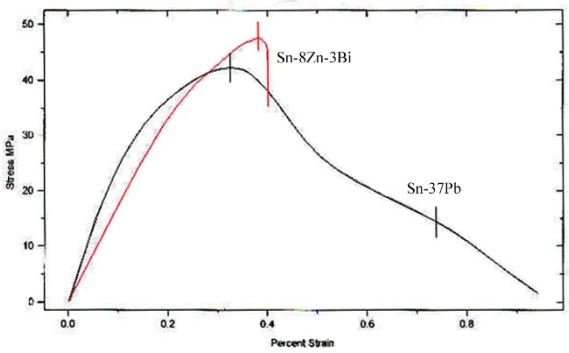

Fig. 8. Stress-Strain curves of solder alloys

The macro image of the broken specimens is shown in Fig. 10.

It can be seen that the solder-substrate joint was broken right at the interface and there is no significant plastic deformation was detected before failure.

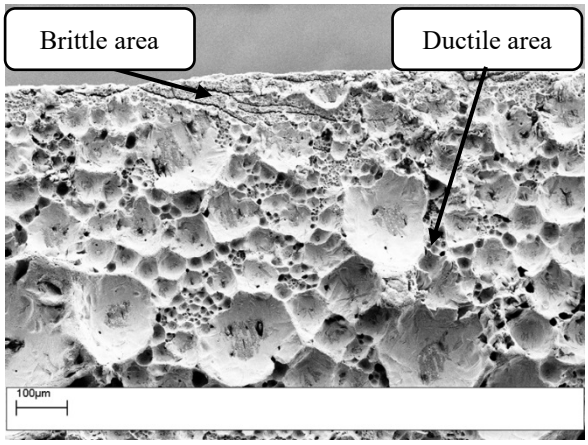

Fig. 9. SEM image of fracture surface

Fig. 10. Broken specimens after tensile testing

3.4 Shear Strength of the Solder Joint

Fig. 11 shows the shear strength of Sn-8Zn-3Bi solder joint in comparison with the Sn-37Pb. The shear strength of the Sn-8Zn-3Bi was found somewhat higher than that of Sn-37Pb. The shear strength of solder alloys was also increased as crosshead speed increased. At 0.1 mm/s of crosshead speed, the shear strength of Sn-8Zn-3Bi was 29.3 MPa and it increased up to 33.6 MPa at a crosshead speed of 1 mm/s. The shear strength of Sn-8Zn-3Bi remains a little higher than Sn-37Pb when crosshead speed changes.

It has been reported that the shear strength of Sn-8Zn-3Bi solder joint was higher than that of Sn-37Pb, the shear strength of Sn-8Zn-3Bi solder joint was as high as 68 MPa [21]. It also reported that the shear strength of the joint is decreasing as the thickness of solder layer increases. The value of 68 MPa was for the joint with the thickness of solder layer is 20 µm [21]. In this work, the thickness of solder layer was around 1 mm, almost 5 times the thickness reported, and thus, resulted in lower shear strength of the solder joint.

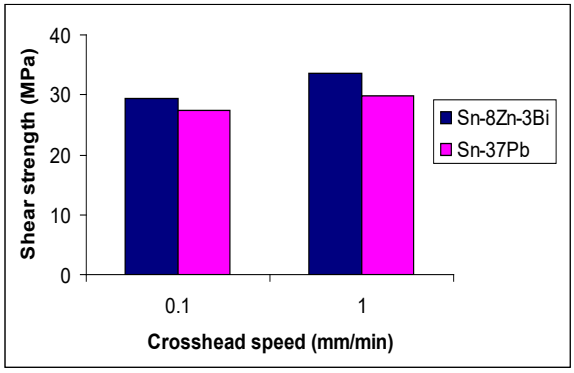

Fig. 11. Shear strength of solder alloys

4. Conclusion

Thermal and mechanical properties of the Sn-8Zn-3Bi solder alloy and the Sn-8Zn-3Bi joints were investigated in order to evaluate the workability of the alloy in comparison with the traditional Sn-37Pb.

The results show that the melting (liquidus) temperature of Sn-8Zn-3Bi was 195 °C, the CTE of Sn-8Zn-3Bi was 22.2×10^{-6} K^{-1} in the temperature range of 30 - 130 °C. At the same testing condition, both tensile and shear strength of Sn-8Zn-3Bi joints were higher than those of Sn-37Pb. The stress-strain curve indicated that the Sn-8Zn-3Bi joints were brittle whilst the Sn-37Pb joints were ductile. The results indicated that the gaps between their melting temperature were relatively small, the melting temperature of Sn-8Zn-3Bi was just approx. 12 °C higher. Such a small gap could be easily overridden in the soldering process and thus, easing the process of replacing Sn-37Pb with Sn-8Zn-3Bi. The Sn-8Zn-3Bi also possesses higher mechanical properties, this is an important factor ensuring the strength of the solder joint. The CTE mismatch between Sn-8Zn-3Bi and Sn-37Pb was also small, this is another factor ensuring the reliability of the joints.

References

[1] Ogunseitan, Oladele A., Public health and environmental benefits of adopting lead-free solders, The Journal of the Minerals, Metals & Materials Society, Vol. 59, pp. 12-17, 2007. https://doi.org/10.1007/s11837-007-0082-8

[2] K.N. Tu and K. Zeng, Tin-lead (SnPb) solder reaction in flip chip technology, Materials Science and Engineering Reports R, Vol. 34, pp. 1-58, 2001. https://doi.org/10.1016/S0927-796X(01)00029-8

[3] Howard H. Manko, Solders and Soldering, 4th edition, New York, USA: McGRAW-HILL, 2001.

[4] Abtew Mulugeta, Selvaduray Guna, Lead-free solders in microelectronic, Materials Science and Engineering Reports, Vol. 27, pp. 95-141, 2000. https://doi.org/10.1016/S0927-796X(00)00010-3

[5] Seung Wook Yoon, Won Kyoung Choi, Hyuck Mo Lee, Calculation of surface tension and wetting properties of sn-based solder alloys, Scripta Materialia, Vol. 40, No. 3, pp. 297-302, 1999. https://doi.org/10.1016/S1359-6462(98)00417-5

[6] Mario F. Arenas, Viola L. Acoff, Contact Angle Measurements of Sn-Ag and Sn-Cu Lead-Free Solders on Copper Substrates, Journal of Electronic Materials Vol. 33, No. 12, pp. 1452-1458, 2004. https://doi.org/10.1007/s11664-004-0086-x

[7] E.A. Howell, C.M. Megaridis, M. McNallan, Dynamic surface tension measurements of molten Sn/Pb solder using oscillating slender elliptical jets, International Journal of Heat and Fluid Flow, Vol. 25, pp. 91-102, 2004. https://doi.org/10.1016/j.ijheatfluidflow.2003.10.003

[8] Mario F. Arenas, Min He, Viola L. Acoff, Effect of flux on the wetting characteristics of SnAg, SnCu, SnAgBi, and SnAgCu lead-free solders on copper substrates, Journal of Electronic Materials, Vol. 35, No. 7, pp. 1530-1536, 2006. https://doi.org/10.1007/s11664-006-0144-7

[9] Jae-Ean Lee, Keun-Soo Kim, Masahiro Inoue, Junxiang Jiang, Katsuaki Suganuma, Effects of Ag and Cu addition on microstructural properties and oxidation resistance of Sn-Zn eutectic alloy, Journal of Alloys and Compounds, Vol. 454, pp. 310-320, 2008. https://doi.org/10.1016/j.jallcom.2006.12.037

[10] H. Y. Guo, J. D. Guo, and J. K. Shang, Influence of thermal cycling on the thermal resistance of solder interfaces, Journal of Electronic Materials, Vol. 38, pp. 2470-2478, 2009. https://doi.org/10.1007/s11664-009-0857-5

[11] H. Mavoori, J. Chin, S. Vaynman, B. Moran, L. Keer, M. Fine, Creep, stress relaxation and plastic deformation in Sn-Ag and Sn-Zn eutectic solders, Journal of Electronic Materials, Vol. 26, pp. 783-790, 1997. https://doi.org/10.1007/s11664-997-0252-z

[12] Song J.M., Lan G.F., Lui T.S., Chen L.H., Microstructure and tensile properties of Sn-9Zn-xAg lead-free solder alloys, Scripta Materialia, Vol. 48, pp. 1047-1051, 2003. https://doi.org/10.1016/S1359-6462(02)00647-4

[13] Chang Tao-Chih, Wang Moo-Chin, Hon Min-Hsiung, Morphology and adhesion strength of the Sn-9Zn-3.5Ag/Cu interface after aging, Journal of Crystal Growth, Vol. 263, pp. 223-231, 2003. https://doi.org/10.1016/j.jcrysgro.2003.05.002

[14] Shohji Ikuo, Gagg Colin, Plumbridge William J., Creep properties of Sn-8Zn-3Bi lead-free alloy, Journal of Electronic Materials, Vol. 33, No. 8, pp. 923-927, 2004. https://doi.org/10.1007/s11664-004-0222-7

[15] Chiu M.Y., Wang S.S., Chuang T.H., Intermetallic compounds formed during interfacial reactions between liquid Sn-8Zn-3Bi solders and Ni substrates, Journal of Electronic Materials, Vol. 31, No. 5, pp. 494-499, 2002. https://doi.org/10.1007/s11664-002-0105-8

[16] Shohji Ikuo, Gagg Colin, Plumbridge William J., Creep properties of Sn-8Zn-3Bi lead-free alloy, Journal of Electronic Materials, Vol. 33, No. 8, pp. 923-927, 2004. https://doi.org/10.1007/s11664-004-0222-7

[17] Duong Ngoc Binh, Contact angle of Sn-8Zn-3Bi lead-free solder alloy on copper substrate, Journal of Science and Technology. Vol. 146, pp. 49-53, 2020. https://doi.org/10.51316/30.7.9

[18] Fleszar M.F., Lead-tin solder characterization by differential scanning calorimetry, Thermochimica Acta, Vol. 367-368, pp. 273-277, 2001. https://doi.org/10.1016/S0040-6031(00)00671-7

[19] Kim K.S., Huh S.H., Suganuma K., Effects of cooling speed on microstructure and tensile properties of Sn-Ag-Cu alloys, Materials Science and Engineering: A, Vol. 333, pp. 106-114, 2002. https://doi.org/10.1016/S0921-5093(01)01828-7

[20] Shohji Ikuo, Yoshida Tomohiro, Takahashi Takehiko, Hioki Susumu, Tensile properties of Sn-Ag based lead-free solders and strain rate sensitivity, Materials Science and Engineering A, Vol. 366, pp. 50-55, 2003. https://doi.org/10.1016/j.msea.2003.09.057

[21] Akio Hirose, Hiroto Yanagawa, Eiichi Ide & Kojiro F. Kobayashi, Joint strength and interfacial microstructure between Sn-Ag-Cu an Sn-Zn-Bi solders and Cu substrate, Science and Technology of Advanced Materials, Vol. 5, No. 1-2, pp. 267-276, 2004. https://doi.org/10.1016/j.stam.2003.10.024